

HARMONIC MAPS OF SURFACES APPROACHING THE BOUNDARY OF MODULI SPACE AND ELIMINATING BUBBLING

SIMON P. MORGAN

ABSTRACT. The limit of energies of a sequence of harmonic maps as their annular domains approach the boundary of moduli space depends upon the boundary point approached. The infinite energy case is associated with limits of images containing ruled surfaces. The finite energy case yields a limit of images, under a suitable topology, with a union of discs and straight line segments. Generalization to higher numbers of boundary components shows that minimal surfaces union straight line segments can still be achieved, and that the configuration of straight line segments depends on the direction of approach of domain conformal classes to the boundary point of domain moduli space. Bubbling can occur in variable ways according to the metric representatives of the conformal classes of domains. A method is given whereby bubbling can be eliminated yielding a point-wise limit of maps with image limit containing a surface union straight line segments.

CONTENTS

1. Introduction	2
2. The annulus example	4
2.1. The one parameter families of domains, images and their limits	4
2.2. Physical intuition I: Lengths of geodesics and domain conformal structure	6
2.3. Defining a common domain for taking limits of maps	7
2.4. Domains represent conformal classes	7
2.5. A topology for image limits.	7
2.6. Image and energy variation	8
2.7. Physical intuition II: Image curvature and energy	9
2.8. Improved energy-image curvature inequality	9
2.9. Examples of moving bubbles around	9
3. Eliminating bubbling in harmonic map sequences.	11
3.1. Physical intuition III: Maps near the identity do not bubble	12
3.2. Constructing metric structures on domains	12
4. Generalizing to more boundary components	14
4.1. Minimal surfaces union straight line segments	14
4.2. Direction of approach to the boundary of moduli space	15
4.3. Physical intuition IV: Force balancing in line segment skeletons.	16
4.4. Parameterized example sequence of domains in moduli space	16
References	16

Key words and phrases. Harmonic maps, bubbling, dimension collapsing.

1. INTRODUCTION

1.0.1. *Example for new compactness theorems.* This paper, the first of two with [MS1], provides an example (Figure 1) of a physical optimization problem involving minimal surfaces and threads of viscoelastic fluids with prescribed boundary and initial conditions.

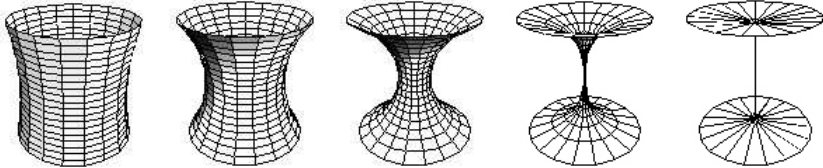


Figure 1: Dimension collapsing

This has a solution which is the limit of minimizers of an energy functional, that is the limit of images of harmonic maps. The regularity associated with minimizers, such as harmonic map images, can help establish existence of limits of such minimizers. The limiting process in our example has two features of interest. First it involves dimension collapsing of the images of the harmonic maps where the lower dimensional sets are part of the solution, under a suitable topology. Secondly discontinuities can arise in bubbling. Although in our examples, each limit of images can be achieved as a continuous point-wise limit by careful construction of a sequence of harmonic maps, in general a sequence will not have a continuous point-wise limit.

The second paper [MS1] provides two versions of a topology that overcome both the problem of requiring the lower dimensional sets to be kept in the limit, and the problem of discontinuities due to bubbling in a sequence of harmonic map images. This is done using sphere bundle measures (in $\mathbb{R}^n \times \mathbb{S}^{n-1}$) to represent sets in \mathbb{R}^n and take limits. The sphere bundle measure compactness has the added advantage of providing a topology which compactifies sufficiently regular unions of rectifiable subsets of \mathbb{R}^n . Fortunately our motivating example consists of taking limits of images of harmonic maps which have sufficient regularity.

1.0.2. *Minimal surfaces union straight line segments.* Douglas [D] showed that minimal surfaces which are topological discs can be images of harmonic maps of fixed discs with some variability in the boundary conditions. We can generalize this method to genus zero minimal surfaces with more than one boundary component by not only varying the boundary conditions, but by varying the conformal class of the domain too.

Consider the case of two boundary components. We take energy minimizing sequences of harmonic maps over varying annular domains. This can result in minimal surfaces union straight line segments as limits of images (figure 1). Such collapsing of surfaces down to line segments are mentioned in the context of harmonic maps [SU] as ‘bridges’ between minimal spheres. In [Fo][DF], where this example is discussed, extraordinary homology is used to define a homology class of solutions that can contain not only surfaces but the limit of surfaces as parts of them collapse down to line segments.

1.0.3. *Harmonic map existence.* The original motivation for the work reported here was to study harmonic maps of surfaces which have singular images such as

cones. In our example these are image limits as the other end of moduli space is approached. This can also be thought of as an inverse problem: What domains can map harmonically onto a given image embedded in Euclidean space? Harmonic maps are solutions to an energy minimizing variational problem with fixed range, domain and boundary conditions. There are many regularity and existence results for harmonic maps, e.g.: [SCU][EL1][EL2][EF].

Sometimes solutions do not exist, even singular ones. Say we wish to achieve an embedded cone as an image of a harmonic map from a disc into \mathbb{R}^3 . If we place boundary conditions on a flat domain disc in \mathbb{R}^3 to be the identity, and also require the center of the disc to be mapped to a point out of the plane, any sequence maps whose energy tends to the infimum will have a point-wise limit with at least one discontinuity as in Figure 2.

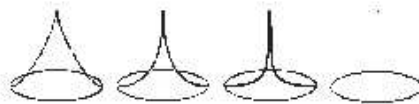


Figure 2: Harmonic map non-existence

Overcoming the non-existence of any harmonic maps for this problem motivated studying maps from annular domains rather than discs. The outer boundary can be mapped to the disc boundary in the range and the inner boundary can be mapped to the point out of the plane. Harmonic maps do exist for this modified problem. However a ruled surface cone can only be achieved as a limit of images of harmonic maps whose energy tends to infinity. See table 1.

1.0.4. **Techniques and bubbling.** We will use two classical results specific to harmonic maps of surfaces. Firstly we use the energy-area inequality for maps of surfaces, $Energy \geq 2(Area\ of\ Image)$ and an improved version (2.4) using image curvature [MS2].

Secondly we use the fact that the image of a harmonic map of a surface is an invariant of the conformal structure of the domain. Any two harmonic maps of surfaces from conformally equivalent domains with compatible boundary conditions will have the same image and the same energy. In our annular domain case, this gives us a one dimensional moduli space of conformal structures which when compactified has two boundary points. This gives us a corresponding 1-parameter family of images with two limits as shown in table 1. See [Ah] and [N] for accounts of the moduli space of multiply connected planar domains.

This invariance of image and energy with respect to domain conformal class means that there are two types of change to domains for harmonic maps of surfaces. Changes of conformal structure, that will in general change the image and energy of a map, and then changes of metric structure within a fixed conformal class. The latter type of changes do not change the image, but can introduce or eliminate the phenomenon of bubbling in sequences of harmonic maps.

We will define bubbling as the phenomenon of a sequence of maps from a fixed domain to a range having a point set limit as a graph but may not necessarily have a point-wise limit as a function because the graph becomes vertical for a set of positive measure in the range. For example the limit as $n \rightarrow \infty$ of the graphs of $f(x) = x^{1/n}$ contains the unit interval on the Y axis. See section 3 for an example of

bubbling with point-wise limits. [SU] gave an early example of bubbling in terms of fractional linear transformations on spheres being conformal, and hence harmonic, but not compact. [W] reviews a variety of research areas where bubbling has to be dealt with.

Consider as an example of bubbling, the sequence of maps from the compactified complex plane to itself, $z \rightarrow nz$. The image of the point-wise limit as $n \rightarrow \infty$ is $\{\infty\} \cup \{0\}$, however the Hausdorff set limit of images is the compactified complex plane. This poses problems for trying to study limits of images of maps as the image of the point-wise limit of a map, as parts of the image can be lost in the limit. Also it may lead to a change in the degree of maps between the limits of images and images of point-wise limits of maps. We eliminate bubbling in section 3 similarly to [SU] where parameterizations are chosen to be ‘in balance’.

The development of minimal surface theory after Douglas included many mathematical approaches, and we shall use one of these in particular, geometric measure theory [S][MF][F]. Federer and Fleming [FF] used current compactness to prove the existence of minimal surfaces in \mathbb{R}^n with certain fixed boundary. We will use varifold and current compactness in a novel way on the sphere bundle [MS1] to take limits of the images. This avoids the problems of bubbling for point-wise limits, and captures lower dimensional sets in the limit. The Hausdorff set topology also has these advantages, but does not ensure the regularity, rectifiability and measurability, given by geometric measure theory.

2. THE ANNULUS EXAMPLE

2.1. The one parameter families of domains, images and their limits.

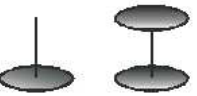
	Domain boundary components	Variations of Domain Annulus	Harmonic map energy	Images and Hausdorff set limits for two fixed sets of boundary conditions	Principle Curvature Ratios
L I M I T	∞ relative distance apart	 infinitely thin cylinder	Local minimum = 2 image area		Formally 1 or undefined on line segments
	Far apart		Low energy		Low ratios on large area
	Close together		High energy		High ratios
L I M I T	Coincident	Degenerates to a circle 	∞ energy		∞

Table 1

Table 1 shows two domain annuli for a harmonic map and their respective images (rows 2 and 3). A geometric interpretation of the two limiting cases of domains and images is given (rows 1 and 4). Note that the energy-area inequality for harmonic maps is true in row 1 of the table, where we do not have a harmonic map but a limit of energies of harmonic maps and a limit of their images. In row 4, the limit of energies is trivially greater than twice the areas of the limits of images. Using (2.4) the first inequality has infinity on both sides for this case.

The images for domains on the interior of moduli space are obtained as solutions (2.2) to an ODE (2.1) based on the first variation of energy of a radially symmetric map $h(x, \theta) = (R(x), \Theta(\theta), Z(x))$, of an annulus based on identified rectangle of width $2\pi/a$, ($0 < \theta < 2\pi$), and height a , ($-a/2 < x < a/2$). For each row in table 1 we can give values of a . See table 2.

Row in Table 1	a
1	∞
2	3
3	0.5
4	0

Table 2

Note: $a \in (0, \infty)$ is a parameter representing the conformal class of the domain annulus.

Let $\varsigma(x)$ be any smooth function with compact support that vanishes on the boundary. We take the derivative of the energy of the deformed family of maps $h(x, \theta) = (R(x) + \varsigma(x)t, \Theta(\theta), Z(x))$, with respect to time and set it equal to zero. Note we are only considering radially symmetric deformations only. The energy can be expressed in terms of squares of the entries of the Jacobian in local orthonormal coordinates yielding:

$$\frac{d}{dt} \Big|_{t=0} \int \left((R_x + \varsigma_x(x)t)^2 + \left(\frac{\partial \Theta}{\partial \theta} \right)^2 (R + \varsigma(x)t)^2 \right) dA = 0$$

After multiplying out, differentiating under the integral sign, using integration by parts, and setting the integrand to zero yields:

$$a^2 R \varsigma(x) - R_{xx} \varsigma(x) = 0$$

This is always satisfied when

$$(2.1) \quad a^2 R - R_{xx} = 0$$

The general solution for the image in cylindrical R, Θ, Z coordinates is of the form;

$$(2.2) \quad R = \frac{A \cosh(a^2 Z)}{\cosh(a^2)} + \frac{B \sinh(a^2 Z)}{\sinh(a^2)}$$

where $a \in (0, \infty)$ is a parameter representing the conformal class of the domain annulus. Also similar calculations show that Z turns out to be a linear function of x , and that the radially symmetric map is energy stationary.

Certain of these hyperbolic catenoids ($B = 0$) will be minimal surfaces (see [MF][Fo][DF] for examples), and these may be stable or unstable. For fixed boundary conditions such minimal surfaces occur only if the boundary circles are sufficiently close together for the given radii.

In higher dimensions harmonic maps from products of spheres and an interval give an analogous solution. A product of an \mathbb{S}^n of radius $\frac{1}{n\sqrt{a}}$ with an interval of length a , will map harmonically into \mathbb{R}^{n+2} with unit \mathbb{S}^n at a distance 1 apart as boundary conditions. Equation (2.2) now generalizes to

$$(2.3) \quad R = \frac{A \cosh\left(na^{1+\frac{1}{n}}Z\right)}{\cosh\left(na^{1+\frac{1}{n}}\right)} + \frac{B \sinh\left(na^{1+\frac{1}{n}}Z\right)}{\sinh\left(na^{1+\frac{1}{n}}\right)}$$

This means that in higher dimensions the same qualitative behavior as depicted in table 1 occurs. The image becomes a cylinder at one limit and a union of a straight line segment and two $n+1$ balls at the other limit. Note also that suitably interpreted, equation 2.3 holds for $n = 0$, giving $R = A$.

2.2. Physical intuition I: Lengths of geodesics and domain conformal structure. The moduli space of a domain surface $([Ah][N])$, is the space of all conformally equivalent structures on the surface. In the case of the domain annuli in table 1, the ratio of height to width of the identified rectangle indicates the conformal structure. The moduli space of the torus minus two discs in figure 3 can be considered in terms of the ratio of lengths of curves connecting distinct pairs of boundary components (a) and curves going round homologically distinct and non-trivial loops (b, c, d, e). Note that some of these can be the boundary curves (d), (f).

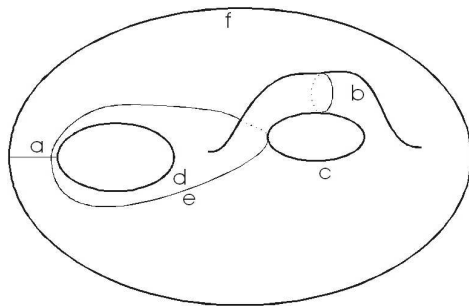


Figure 3: Curve lengths represent position in moduli space

Returning to our annular domain metric structure varying with fixed compact range and boundary conditions from, table 1. As one length becomes longer in the domain, we care less about the length of its image, as the corresponding Jacobian entries will be small anyway. As it becomes shorter then we care more about its length in the image, as we can make big savings on energy (integral of sum of squares of Jacobian entries) by reducing the value of the corresponding Jacobian entries when their values are high. So when the domain becomes a thin cylinder we care about shrinking the circles in the image and do not care about the length of curves that connect boundary components. Hence the image collapses down to line segments along the axis of rotation union discs at the boundary components.

Similarly when the domain becomes a thin ribbon, almost a circle, the distance between boundary components in the domain is very short so we care about making the distance between boundary components in the image short. The corresponding Jacobian entries will be large, because the boundary components in the range are a fixed distance apart. Conversely we care less about the length of the meridian circles in the image. Hence in the limit the images become ruled surfaces in this example with geodesics in \mathbb{R}^3 connecting the boundaries. The fact that these entries must go to infinity when the domain distances become small makes the energy go to infinity at this type of limit of moduli space.

To summarize, in limiting behaviors, proportionately longer curves in the domain get mapped to longer curves in the image and proportionately shorter curves in the domain get mapped to shorter curves in the image that can collapse to a point if they bound a disc in the range.

2.3. Defining a common domain for taking limits of maps. We need topologies for the limits of domains, maps and images as $a \rightarrow 0$ and $a \rightarrow \infty$. For the domain limits as shown in table 1, we cannot use the Hausdorff set topology inherited from the metric of the intervals $[-a^2, a^2] \times [0, 2\pi] \in \mathbb{R}^2$ because these sets are unbounded. Instead we can use it if we take a uniformly compact representative of each conformal class such as $[-a^2, a^2] \times [0, 2\pi]$ for $a \rightarrow 0$ and $[-1, 1] \times [0, 2\pi/a^2]$ for $a \rightarrow \infty$.

For technical reasons we need to treat these domains as a fixed annulus $[-1, 1] \times [0, 1]$ with a varying metric;

$$g(a)_{ij} = \begin{bmatrix} a^2 & 0 \\ 0 & 2\pi \end{bmatrix} g_{ij}, \text{ for } a \rightarrow 0 \text{ and } g(a)_{ij} = \begin{bmatrix} 1 & 0 \\ 0 & \frac{2\pi}{a^2} \end{bmatrix} g_{ij}, \text{ for } a \rightarrow \infty$$

Denote the domain limits d_0 and d_∞ respectively. We can now define the matrices as deformations f_i such that $d_i = f_i(d_1)$. This defines $h_i \circ f_i$ the pull-back maps of the harmonic maps to the fixed domain d_1 , $[-1, 1], [0, 2\pi]$, enabling point-wise limits to be taken. When bubbling occurs the point-wise limit map's image will be a subset of the Hausdorff set limit of the images.

2.4. Domains represent conformal classes. However, to be precise, we are really interested in the map H from the space of conformal classes C_a in moduli space D of the domain to an image set X in the range. Here a is the a in table 2 which indicates conformal class. So $image(h(d_a))$ is the image set of a harmonic map h from metric representative d_a of conformal class C_a . The image and energy of h is an invariant of C_a .

Definition 2.1. $H : C_a \rightarrow X \Leftrightarrow \forall d_a \in C_a, image(h(d_a)) = X$

In this case the limit would result from combining the above domain and range limits, enabling us to extend H to C_0 and C_∞ , the boundary points of moduli space where $a = 0$ and $a = \infty$ in section 2.1.

Definition 2.2. $\overline{H} : C_a \rightarrow X \Leftrightarrow \lim_{a \rightarrow i} (image(h(d_a)))$ for $i \in [0, \infty]$

2.5. A topology for image limits. In this section we outline a new technique [MS1] for taking limits of surfaces using geometric measure theory on the sphere bundle of \mathbb{R}^3 . This gives us rectifiable sets as limits of rectifiable sets and captures lower dimensional sets that arise in the limit such as those resulting from surfaces collapsing down curves or points. Consider the canonical example of a sequence of

circles in \mathbb{R}^2 of radii tending to zero. Their lift in the sphere bundle will tend to a line, see figure 4. This projects down a positive measure concentrated at a point.

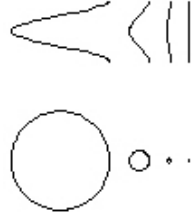


Figure 4: A sequence (below) and its lift (above)

2.6. Image and energy variation. We recall the qualitative observation on how deforming the domain to different limits in moduli space will either make energy finite or infinite. For this section we will consider domains $d_a = [-a, a] \times [0, \frac{2\pi}{a}]$.

2.6.1. High energy ($a \rightarrow 0$). We keep domain area constant, so energy depends on the average sum of squares of entries of the Jacobian. When $a \rightarrow 0$, the two boundaries of the domain annulus become very close. This requires a very high energy for the image to span the boundary conditions in \mathbb{R}^3 .

2.6.2. Low energy ($a \rightarrow \infty$). Conversely as $a \rightarrow \infty$, the boundaries become far apart in the domain, enabling energy to be minimized or to stay finite as the Jacobian entries will mostly be small. However this finite energy limit can exhibit bubbling, and the image will collapse down to a line segment union one or two discs.

Notice that in the low energy limit in table 1, the energy limits equal twice the area of the minimal surfaces in the corresponding limits of the images. This motivates extending the classical energy-area inequality to the limits of maps. Note also that the inequality can be expressed in terms of H above, as well as \bar{H} , making its statement extendable.

Note that the energy minimizer under domain deformation may or may not be at the boundary of moduli space, depending on the boundary conditions in the range. For example if the minimal surface catenoid connecting two boundary components has lower area than the two discs, then the conformal structure on the interior of moduli space that maps to the catenoid by a harmonic map will yield the energy minimizer.

Also note that in the finite energy limit the tubes which collapse down to straight line segments do not contribute to the energy as they have zero area. This is of interest as the next section shows that the entries of the Jacobian that contribute to energy will go to infinity in a thin tube.

This allows a generalization of Douglas' result for existence of certain minimal surfaces as images of harmonic maps from discs. Douglas takes the minimum energy map over a disc with fixed conformal structure as boundary values vary. If instead we allow the domains to have topology and hence non trivial moduli space, we can find the energy minimizer for maps to multiple boundary conditions, as conformal structure of domain and boundary values vary. The thin tubes with zero energy in the limit allow for the image limit to be unions of minimal surfaces, with separate boundary conditions, connected by straight line segments.

2.6.3. Energy and image curvature. Note that at the ‘high energy maps’ end of moduli space, in our example, the energy goes to infinity as the image approaches a cylinder or a cone. These have one principle curvature positive finite and the other zero. This suggests a relationship between ratios of principle curvatures, and energy of harmonic maps, as they can both tend to infinity together, giving ruled surface image limits. Similarly at the low energy end we have minimal surface image limits, and principle curvature ratios =1. Thus both quantities are minimized together.

This observation, that the ratio of principle curvatures in an image can lead to infinite energy maps, implies that the inverse problem mentioned in the introduction may not always have a solution. We can now quote a physical intuition and result from [MS2]

2.7. Physical intuition II: Image curvature and energy. Also we can say that as the image deviates more from being a minimal surface, more energy is required of the harmonic map. A physical interpretation is to consider an elastic sheet with low curvature in one direction and high curvature in the other. To maintain equilibrium, the tension in the sheet in the low curvature direction must be much greater than in the other direction, thus contributing more to energy. This effect can be seen in the infinite energy ruled surface cases, cone and cylinder, in table 1, where the principle curvature ratios go to infinity.

This can also be extended to the case of a planar sheet with higher in tension in one direction than in another. If we consider small deformations of the boundary data, then small curvatures will be introduced into the sheet and their ratios will reflect the ratios in the tensions in different directions.

2.8. Improved energy-image curvature inequality.

Theorem 2.3. *If h is a degree 1 harmonic map from a smooth compact surface into \mathbb{R}^n , and ρ_1 and ρ_2 are principle curvatures of the image of h , then*

$$(2.4) \quad \text{Energy} \geq \iint_{\text{image}} \left(\sqrt{\frac{\rho_1}{\rho_2}} + \sqrt{\frac{\rho_2}{\rho_1}} \right) d_i d_j \geq 2(\text{area of image})$$

whenever the integral makes sense on the image taking $\frac{0}{0} = 1$.

Furthermore when the pull back to the domain of the directions of principle curvatures are defined, we can say that equality is achieved on the left hand side if and only if the pull back of the directions of principle curvatures are orthogonal in the domain. This occurs for the radially symmetric case.

When $\rho_1 = \rho_2$, the right hand side becomes twice the area of the image. For proof of the inequality see [MS2].

2.9. Examples of moving bubbles around. Here are four parameterizations in terms of s and θ , of the annuli under domain deformations with the metrics inherited from Euclidean space in the obvious way. The point-wise image limit is shown in Table 3. The bubble in each case being the discs union the straight line segment minus the image shown. Each domain is parameterized in terms of a fixed annulus $A = \{(s, \theta) : (s, 0) = (s, 2\pi), -1 \leq s \leq 1, 0 \leq \theta \leq 2\pi\}$. Now first we have the parameterization of the domain $D_\varepsilon = u_\varepsilon(A)$. The harmonic map $h : D_\varepsilon \rightarrow \mathbb{R}^3$. Note that u is always uniformly bi-Lipschitz for each ε .

1) D_ε is an identified rectangle in \mathbb{R}^2 plane, given by $u_\varepsilon : (s, \theta) \rightarrow (x, y)$, $x = s$, $y = \varepsilon\theta$.

Here the point-wise limit of $h(u_\varepsilon(s, \theta)) \rightarrow (R, \Theta, Z)$ as $\varepsilon \rightarrow 0$, the pull backs of the harmonic maps as $\varepsilon \rightarrow 0$ is given by $f(s, \theta) \equiv \left\{ \begin{array}{l} (1, \theta, 0) \text{ for } s = 0 \\ (0, \theta, s) \text{ for } 0 < s < 1 \\ (1, \theta, 1) \text{ for } s = 1 \end{array} \right\}$ where the mass (two dimensional Hausdorff measure) of the domain is mapped to the line segment, and the disc interiors bubble.

2) D_ε is the planar annulus. In polar coordinates $r = \varepsilon + s(1 - \varepsilon)$, $z = 0$. Here the point-wise limit of the pull backs of the harmonic maps as $\varepsilon \rightarrow 0$ is given by $f(s, \theta) \equiv \left\{ \begin{array}{l} (1, \theta, 0) \text{ for } s = 0 \\ (1, \theta, 1) \text{ for } s > 0 \end{array} \right\}$

Here the bubble is one boundary ring, the interiors of the two discs and the straight line segment.

3) The double cone/hyperboloid with a metric from cylindrical coordinates in \mathbb{R}^3 given by $z^2 = r^2 + \varepsilon$, $-1 < z < 1$. Here the point-wise limit of the pull backs of the harmonic maps as $\varepsilon \rightarrow 0$ is given by $f(s, \theta) \equiv \left\{ \begin{array}{l} (1, \theta, 0) \text{ for } s < 0.5 \\ (0, \theta, 0.5) \text{ for } s = 0.5 \\ (1, \theta, 1) \text{ for } s > 0.5 \end{array} \right\}$

Here the bubble is the interiors of the two discs and the straight line segment minus the center point.

4) The spherical annulus. That is an annulus in spherical coordinates with $\rho = \varepsilon + s(\pi - \varepsilon)$, with metric inherited from \mathbb{R}^3 . Here the point-wise limit of the pull backs of the harmonic maps as $\varepsilon \rightarrow 0$ is

$$f(s, \theta) \equiv \left\{ \begin{array}{l} (1, \theta, 0) \text{ for } s = 0 \\ (0, \theta, 0.5) \text{ for } 0 < s < 1 \\ (1, \theta, 1) \text{ for } s = 1 \end{array} \right\}$$

Here the bubble is the interiors of the two discs and the straight line segment minus the center point.

To derive these results consider a conformal map from each D_ε to an annulus in the shape of part of the surface of a cylinder. This involves the identity on θ , and scaling the longitudinal directions along the surface by $\frac{1}{r}$ to give a conformal map. Then h will map the longitudinal direction linearly onto Z . Equation 2.2 then gives the $R(Z)$ coordinate, with $\Theta = \theta$.

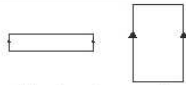
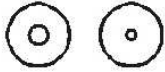
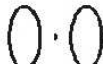
Parameterized domain with inherited Euclidean metric	Images of point-wise limit and where mass is mapped
 <p data-bbox="565 468 716 489">Rectangular annuli</p>	 <p data-bbox="805 453 1092 495">Parameterized domain with inherited Euclidean metric</p>
 <p data-bbox="586 596 725 617">Planar annuli</p>	 <p data-bbox="841 596 1052 617">Mass on one Boundary ring</p>
 <p data-bbox="553 726 737 747">Truncated hyperboloids</p>	 <p data-bbox="857 716 1040 737">Mass on boundary rings</p>
 <p data-bbox="521 831 758 852">Spheres minus antipodal discs</p>	 <p data-bbox="867 833 1029 854">Mass on center point</p>

Table 3: Examples of bubbling

We can move the bubble and discontinuity around, from row to row in table 3, by changing the metric representatives of the conformal classes of domain. The next section uses this flexibility to eliminate bubbling by making the domain metric limit close to the limit image metric, and invoking a compactness theorem [MS1] applicable to sets with the regularity of images of harmonic maps in Riemannian manifolds.

3. ELIMINATING BUBBLING IN HARMONIC MAP SEQUENCES.

Bubbling is the phenomenon of limits of maps where, if we consider the limit of the graphs of the maps, a region of the image lies over a lower dimensional region of the domain. In the case of sequences of harmonic maps with varying domains we have to set up a fixed domain to be able to talk about bubbling. In section 2.3 we composed the harmonic maps with the unique linear map from the identified unit square to the domains of the harmonic maps.

In our examples from table 1 bubbling is always associated with a discontinuity in the point-wise limit. In general this need not happen with bubbling, but bubbling cannot occur without derivatives becoming unbounded as relatively smaller parts of the domain are mapped to larger parts of the image. Consider the limit of functions: $\lim_{n \rightarrow \infty} (nxe^{-(nx)^2})$. The point-wise limit is zero everywhere, despite there being a bubble.

However we will see in certain cases that if we construct a sequence of domain metrics that tend to the limit in the same way as the metric structures of the images, then we do not have bubbling. First we will consider more general cases before giving an outline of the proof for the radially symmetric case.

3.1. Physical intuition III: Maps near the identity do not bubble. Aiming to make the limit of maps like the identity map may minimize energy in some sense and eliminate bubbling, by aiming to keep derivatives bounded near to 1.

3.2. Constructing metric structures on domains. Allow the domains D_n and Images I_n to be topologically equivalent; e.g.: an annulus as in section 2. Then we can define a condition to avoid bubbling by comparing the metrics on the domains and images. To enable comparison, we set up pull back metrics from both domains and ranges on a topologically equivalent manifold M via the maps, $\Psi_{D_n} : M \rightarrow D_n$ and $\Psi_{I_n} : M \rightarrow I_n$ giving $d_{D_n}(x, y) = d(\Psi_{D_n}(x), \Psi_{D_n}(y)), \forall x, y \in M$ for the domains and similarly for the images. Thus the no-bubbling condition can be defined as:

$$\lim_{n \rightarrow \infty} d_{D_n}(x, y) = \lim_{n \rightarrow \infty} d_{I_n}(x, y), \forall x, y \in M \quad (\text{Condition 3.1})$$

Note that in the dimension collapsing case these limits can be zero. Bubbling involves unbounded distance ratios between points in the domain and the range. This is impossible in the above condition. The following lemmas show that the limits of the graphs will be the identity, in suitable coordinate systems. Lemmas 3.1 and 3.2 develop this idea, and allow us to state theorem 3.3 which is developed further in special cases in theorem 3.4.

Lemma 3.1. (*special case*)

The identity map from a surface to a surface is harmonic, when the surface is the range.

Proof. This is because energy will equal twice the area, giving equality for the energy inequality, and achieving the minimum possible. \square

Lemma 3.2. *If two sequences of metrics, $d_{1,i}$ and $d_{2,i}$, on a surface are close in the sense that a bi-Lipschitz bijection exists between them with Lipschitz constants less than $1 + \varepsilon$, ($0 < \varepsilon < 1/i$), then such bijections will have energy that tends to twice the area of the image as $\varepsilon \rightarrow 0$.*

Proof. From the bi-Lipschitz condition we can write:

$$\frac{(\text{area of image})}{(1+\varepsilon)^2} \leq (\text{area of domain}) \leq (\text{area of image})(1+\varepsilon)^2.$$

Now $\text{Energy} \leq 2(\text{area of domain})(1+\varepsilon)^2$ by definition of energy. These combine to give $\text{Energy} \leq 2(\text{area of image})(1+\varepsilon)^4$. As $\varepsilon \rightarrow 0$ we approach the desired equality, as $\text{Energy} \geq 2(\text{area of image})$ for any map of surfaces. \square

As the image only depends on the conformal class of the domain, we can then choose the metric representatives, d_{D_n} in the sequence to satisfy condition 3.1. We can now conclude:

Theorem 3.3. *Suppose the hypotheses for lemma 3.2 are satisfied by a sequence of domains and images of a sequence of harmonic maps which themselves need not be uniformly bi-Lipschitz. Then we can set up a sequence of uniformly bi-Lipschitz maps with energy and image tending to the same limits as the energies and images of the original harmonic map sequence.*

The proof follows from Lemma 3.2. We will prove a stronger theorem in the special case of our radially symmetric examples from section 2.

Theorem 3.4. *When the hypotheses for lemma 3.3 are satisfied in the radially symmetric case with annular domains the new sequence in the conclusion of theorem 3.3 can be chosen to be a sequence of harmonic maps.*

We construct a set of domains that approaches the limit image, as suggested by thm. 3.2. See figure 5. Two annuli connected by a thin tube are given dimensions to fit the boundary data in \mathbb{R}^3 . As $\varepsilon \rightarrow 0$, the boundary of moduli space is approached and the domain approaches the image limit.

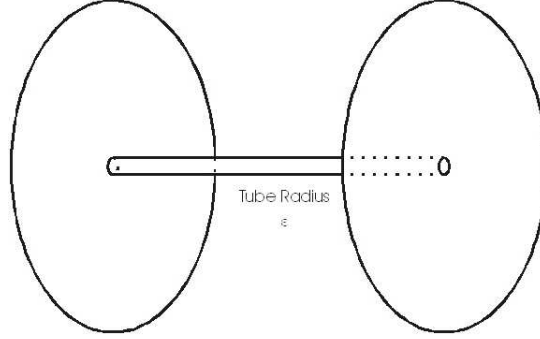


Figure 5: Domains to eliminate bubbling

Proof. Given symmetric boundary data we know that the image will satisfy equation 2.2. As we approach the boundary of moduli space in the domain we can show that in our approximation to the image, the tube is mapped mainly to the tube and the punctured discs are mapped mainly to the punctured discs. We do this by making energy calculations for small thin annuli near the puncture of the discs in figure 5.

Part 1: Tubes do not fan out into the annuli.

Consider an annulus in the domain of inner radius r , and outer radius $2r$ centered on the axis. Lets say it maps to a radius of at least k . The map has a tangential derivative of at least $\frac{k}{2r}$, and so the energy for this small annulus is at least $\left(\frac{k}{2r}\right)^2 3\pi r^2 = \frac{3\pi k^2}{4}$. However as $\varepsilon \rightarrow 0$, we need an infinite number of such annuli of radii $\frac{r}{2^n}$, so the energy becomes infinite, unless there is no such $k > 0$ that the tubes fan out to.

Part 2: The annuli do not stretch into the tubes.

We calculate the image of the neck of the tubes. First we need to conformally map a domain such as that in figure 5 to an identified rectangle annulus as in table 1. Let this annulus be a cylindrical surface of circumference 2π , and let the domain, without loss of generality, have length 1 and boundary radii 1. The conformal map will scale the length along the cylinder by the reciprocal of the radius of the domain.

Each planar annulus in figure 5 will be mapped to a length of $|\log(\varepsilon)|$. This is explained in the final paragraph of section 2.9. The tube part in figure 5 will be mapped to a length of $\frac{1}{\varepsilon}$. We know from section 2.1 that Z (varies from -1 to 1) is a linear function of x (varies from $-|\log(\varepsilon)| + \frac{1}{2\varepsilon}$ to $|\log(\varepsilon)| + \frac{1}{2\varepsilon}$), so we can place the image of one of the necks at $1 - \left(\frac{|\log(\varepsilon)|}{|\log(\varepsilon)| + \frac{1}{\varepsilon}}\right)$. As $\varepsilon \rightarrow 0$, this becomes 1. Therefore the images of the necks remain at the ends of the tube as required. We have shown that the sequence of harmonic maps tend to the identity and so do its derivatives. It satisfies condition 3.1, therefore it does not bubble. \square

Conjecture 1. *Whenever the domain deformation and induced image variation tend to the same boundary point of moduli space we can eliminate bubbling by choice of domain representatives of conformal classes, and if needed by choice of harmonic map. [MS1] gives a topology in which images of harmonic maps converge to give the desired limit image with dimension collapsing. This limit image can then be used to construct a set of domains which will lead to a sequence of harmonic maps which converge point-wise to the limit image.*

Theorem 3.5. *For the construction in thm 4.1 conjecture 1 is true*

Proof. As proof for thm 3.4 □

4. GENERALIZING TO MORE BOUNDARY COMPONENTS

4.1. Minimal surfaces union straight line segments. The following theorem was conjectured by Robert Hardt.

Theorem 4.1. *For connected planar (genus zero) multiply connected domains with more than 2 boundary components, there will be a sequence of harmonic maps from domains approaching a boundary point in moduli space whose energies approach the infimum of all energies of harmonic maps from that topological type of surface over all conformal structures with range \mathbb{R}^n and a union of suitably embedded \mathbb{S}^1 s as Douglas type boundary conditions. Furthermore the limit of images under a suitable topology that captures dimension collapsing such as in [MS1] will be a union of minimal surfaces interconnected by an embedded complex of straight line segments.*

We construct a domain consisting of n planar annuli each connected by a thin tube of length 1 and diameter ε . These tubes meet in a central joint, so that the whole domain has the topological type of an \mathbb{S}^2 with n discs removed. The sequence of domains is given by $\varepsilon \rightarrow 0$. Douglas boundary conditions are used for technical reasons.

Theorem 4.2. *We know that every section of two tubes connecting any pair of boundary components will pinch down to an arbitrarily small diameter at least one point.*

Proof. This is because if it does not, the energy on that section of tubes will grow to the order of $\frac{1}{\varepsilon}$ as $\varepsilon \rightarrow 0$. □

Proposition 1. *This means at least $n-1$ tubes contain a pinch, even if they all pinch at the joint.*

Proposition 2. *The images of harmonic maps as $\varepsilon \rightarrow 0$ contain annuli contained in the convex hull of each boundary component and a circle diameter ε embedded in \mathbb{R}^n .*

Proof. The convex hull property of images of harmonic maps applies between the neck pinch and the boundary component. □

Proposition 3. *As $\varepsilon \rightarrow 0$ the image area measure will tend to the sum of the areas of minimal surfaces each with one of the prescribed boundary components*

Proof. For a given conformal class with ε small we can show that the area of the annular part of the image is within a fixed range of the area A of the minimal surface bounded by the boundary component. We do this by constructing a candidate

image with $energy \leq 2A + e(\varepsilon)$, where e is arbitrarily small. We know by the area-energy inequality that the area of the actual image A' is within $e/2$ of A . The candidate images are the minimal surfaces each with a disc removed (from Douglas' result [D]) and a tube of diameter ε attached leading to a common ball of diameter 2ε where the tubes join with the required topology. \square

Proof. (of **theorem 4.1**) A deviation from the minimal surface can only be achieved by thin immersed tubes. The topology of the domain ensures that such thin tubes will be retractable, in an appropriate sense for immersed tubes, to the surface, apart from the ones required by domain topology. The retraction in each case can be done so as to decrease energy of the map. The tubes will be straight line segments by the convex hull property of images of harmonic maps. \square

Conjecture 2. *It may even be possible that there is only one boundary point of a suitably compactified moduli space which has a finite energy limit of map energies for a given set of minimal surfaces spanning boundary components.*

We need to specify the set of minimal surfaces, to apply theorems, as there may be more than one. In particular consider the annulus example. In addition to the two discs there can be one or even two catenoids with the same boundary conditions. In the annular examples these catenoids do not occur as images at the boundary of moduli space, but in the higher boundary component case they can.

We can observe that in these cases, of higher dimensional moduli space we can consider not only the boundary point of moduli space approached by a sequence of domains but also the direction of approach of the sequence within higher dimensional moduli space. We should also recall that the choice of metric representative of conformal class can be used to eliminate bubbling, by use of domains with both discs and thin tubes.

4.2. Direction of approach to the boundary of moduli space.

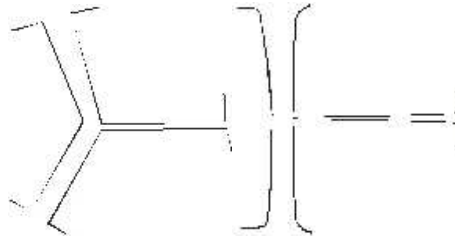


Figure 6 Domain and Image in cross section

Conjecture 3. *The surface parts of the limit image will depend only upon the boundary point of moduli space approached, but the complex of straight line segments can depend also upon the direction of approach of a sequence, or subsequence with a convergent image under a topology such as in [MS1].*

Consider the example of three boundary components. The moduli space of the domains will be more than one dimensional. This means that boundary points of moduli space can be approached by a sequence in different directions on a surface, so we can investigate if the limit of images of harmonic maps depends on just the boundary point or the way it is approached within moduli space.

We give a conjectured example in figure 6 that show the direction of approach to the boundary of moduli space of a sequence of domains making a difference. We will try to support this with a physical intuition and also a parameterization.

4.3. Physical intuition IV: Force balancing in line segment skeletons.

Three line segments meeting at a point where their forces balance will form some kind of Y. If all the forces are equal then all the angles will be equal. If one of the forces is significantly less then the angle in the other two will lie in $[\pi/3, \pi/2)$.

This models what happens at the finite energy boundary of moduli space. If one of the domain tubes in figure 6 shrinks in radius more quickly than the rest, with length constant, then it will act like the line segment with less force. The limit angle in $[\pi/3, \pi/2)$ will depend upon these ratios, when they are constant, which are associated with a different path in moduli space. In this case the limit can be expressed as a stationary varifold. In fact we can even obtain a T-junction as a limit using a diagonalization argument having the ratios change. Note that a T-junction cannot be achieved by a three line segments balancing non-zero forces, i.e. they cannot be represented as a stationary varifold.

4.4. Parameterized example sequence of domains in moduli space.

We suggest the case of the T-junction as a limit of images of harmonic maps could perhaps be achieved by a sequence of domains that must approach the boundary of moduli space tangentially. Let x, y, z be the respective radii of the three tubes of unit length that are all connected at one end in a small punctured sphere in a Y-junction. We know the moduli space is three dimensional as the number parameters it has is $3n - 6$ where n is the connectivity or number of boundary components for $n > 2$ [Ah, section 5.1]. The compactified moduli space, is modelled by the positive octant. The origin is the boundary point to be approached. If we approach on the plane $x = y$ we can approach along the path (t, t, kt) where $k > 0$ and t goes to zero. This will give a Y-singularity where the angles depend on k . If we allow k to vary, we can let $k \rightarrow 0$ as $t \rightarrow 0$, giving us a T-singularity or if $k \rightarrow \infty$ we simply get two line segments connecting the three discs.

REFERENCES

- [Ah] Ahlfors, L. *Complex Analysis*. McGraw Hill 1979
- [D] Douglas, Jesse. Solution of the problem of Plateau. *Trans. AMS* 33 (1931), 263-321.
- [DF] Dao, Trong Thi, Fomenko, A.T. *Minimal surfaces, stratified multivarifolds, and the plateau problem*. Translations of mathematical monographs, AMS. vol 84 1991.
- [EF] Eells, J. and Fuglede, B. *Harmonic maps between Riemannian polyhedra*. Cambridge tracts in mathematics no. 142. Cambridge University Press, 2001
- [EL1] Eells, J. and Lemaire, L.: A report on harmonic maps, *Bulletin of the London Mathematical Society* 20 (1988), no. 5, 385-524.
- [EL2] Eells, J. and Lemaire, L.: Another report on harmonic maps, *Bulletin of the London Mathematical Society* 10 (1978), no. 1, 1-68.
- [F] Federer, H: *Geometric measure theory*. Springer-Verlag. reprinted 1996 (reprint of 1996 edition)
- [FF] Federer, H. and Fleming, W. Normal and integral currents, *Annals of Math*, 72 (1960), 458-520.
- [Fo] Fomenko, A.T. *The Plateau Problem: Part II the present state of the theory*. Chapter 4. Studies in the Development of Modern Mathematics Volume 1. Gordon and Breach 1990
- [J] Jost, J. Two-dimensional Geometric Variational Problems. *Annals of Math. Studies*. 1988. Also John Wiley and Sons 1991.
- [MF] Morgan, Frank. *Geometric Measure theory: A beginner's guide*. Academic Press, 2000

- [MS1] Morgan, Simon. *Mixed Dimensional Compactness with Dimension Collapsing from S^{n-1} Bundle Measures*. Preprint.(2004) <http://www.arxiv.org/ps/math.DG/0409065>.
- [MS2] Morgan, Simon. *Improving the Harmonic Map Energy-Area Inequality Using Image Curvature*. Preprint. <http://www.arxiv.org/ps/math.DG/0407499>.
- [N] Nehari, Z. *Conformal Mapping*. Dover 1952 (Chapter 7 on multiply connected domains)
- [S] Simon, L (1984) *Lectures on Geometric Measure Theory* in Proceedings of the Australian National University, Volume3, 1983
- [SU] Sacks, J, and Uhlenbeck, K. The existence of minimal immersions of 2-spheres. *Annals of Mathematics* (1981), 113, 1-24
- [SCU] Schoen, R and Uhlenbeck, K. A regularity theory for harmonic maps. *Journal of Differential Geometry* 17 (1982) no2,307-335.
- [W] Wolfson, J. Gromov's Compactness of pseudo-holomorphic curves. *Journal of Differential Geometry*, 28 (1988) 383-405.

Acknowledgements

Thanks to Bob Hardt who advised my thesis work, part of which is reported in this paper, and also to Mike Wolf for his enthusiastic help. Thanks to Bob Gulliver who helped with supplementary work and guidance for this paper. I also thank Thierry de Pauw, Chun-chi Lin and Qinglan Xia for their discussions on geometric measure theory over the years.

UNIVERSITY OF MINNESOTA
E-mail address: morgan@math.umn.edu
URL: <http://www.math.umn.edu/~morgan>